CHARACTERIZATION OF 3D PRINTING FILAMENTS APPLIED IN RESTORATION OF SENSITIVE ARCHAEOLOGICAL OBJECTS USING RAPID PROTOTYPING

Abstract

Purpose

The aim of this work is to characterize three-dimensional (3D) printing filaments commonly used in Fused Deposition Modeling (FDM) in order to determine their viability for restoration and conservation treatments.

Design

Eight current filaments for FDM from six polymeric materials have been characterized in order to determine their suitability for restoration and conservation treatments. For testing these filaments, specimens are printed with acrylonitrile-butadiene-styrene (ABS); polylactic acid (PLA); polylactic acid with $CaCO_3$ (E.P.); polyethylene terephthalate glycol (PETG); polypropylene (PP); and high-impact polystyrene (HIPS). Suitability of a filament was verified using the Oddy test by detecting the action of volatile pollutants released from the filaments. The morphological and color changes were observed after allowing them to degrade under the exposure of UV radiation. The samples were then analyzed using Fourier-transform infrared spectroscopy (FT-IR). In addition, gas chromatography-mass spectroscopy technique was applied to complete the characterization of the printed filaments.

Findings

Materials investigated are suitable for restoration purposes ensuring long-term stability. Rapid prototyping using FDM is appropriate for restoring sensitive archaeological objects allowing reconstruction of parts and decreasing risk while manipulating delicate artifacts.

Originality

Rapid prototyping using FDM was chosen for the restoration of a fragile and sensitive archaeological glass bowl from Manises Ceramic Museum.

Keywords: Rapid prototyping, Restoration, Archaeological objects, Stability, Conservation of glass.

Paper type: Research paper.

1.Introduction

Three-dimensional (3D) technologies have been frequently used to assist virtual restoration of cultural objects and to create tangible reproductions for dissemination or exhibition purposes. Certainly, rapid prototyping is a technique that has been recently used in replacement of the traditional ones as it offers great advantages by minimizing the risk of deterioration of the object while performing restoration. It can be used to restore archaeological artifacts by modeling and printing the missing fragments that are not found during an excavation. The 3D printed parts can later be incorporated to the gaps corresponding to the missing fragments in the ancient object. Furthermore, this type of restoration facilitates its systematic reproduction when restored pieces have become timeworn and substitution is necessary.

The FDM technique

In recent years, the Fused Deposition Modeling (FDM) technology has not only become one of the most widely used rapid prototyping methods in industries but it has also become significantly popular amongst various kinds of users to perform different applications, hence exhibiting its versatility. There are numerous studies in which FDM has been used in Cultural Heritage

(Alemanno, *et al.*, 2014; Zang, *et al*., 2015*;* Seixas*, et al.*, 2016; Tucci, *et al*., 2017; Balletti , *et al*., 2017). Nonetheless, FDM is not the only technique that can be used to produce objects for cultural heritage purposes. Granular material binding or photopolymerization (Scopigno, *et al*., 2014; Vatani and Choi, 2015) are other types of additive techniques that can be used for this purpose. These other techniques can provide greater accuracy compared with the FDM technique and can produce missing fragments which have a more natural appearance. However, the principal aim of cultural heritage restoration is preserving artifacts from deterioration. This point is extremely important and, during restoration, the main efforts should focus in this direction. In this sense, FDM can be an excellent option as the nature and properties of the filaments used seem to be suitable with many inorganic excavated objects. One important drawback is that commercial filament composition is generally unknown, and for this reason, we cannot assure if those materials are reliable for archaeological restoration. Characterization of 3D printing filaments used for restoration of archaeological objects is a problem that must be investigated in order to ensure their reliability (Cantrell, *et al.*, 2016; Grasso, *et al.*, 2018; Yang, *et al*., 2018; Soares, *et al*., 2018; Behzadnasab, *et al*., 2019; Schwartz, et al*., 2020)*.

Restoring

From the previous discussion it can be understood that while restoring archaeological objects, it is important to know which filament is used as it can affect the conservation treatment when degradation occurs. The results can be compared to those obtained by traditional manufacturing restoration. In fact, the FDM technique is offered as an alternative treatment because the archaeological object is replaced by its virtual model at all stages of the process after the 3D data capture. In glass restoration, FDM avoids putting the fragility of an object at risk.

When restoring archaeological glass, transparency is considered for possible materials. In some cases, new glass is modeled and used as a gap filler material, but these interventions have fragility as a major drawback. Using materials for restoration of ceramic pieces such as plaster is an alternative, despite the fact that it does not meet the transparency requirement. Plaster of paris is the most popular material used for ceramic or stony restoration due to its many advantages. However, if the artifact has a different nature than that of the filler material or if it is made up of glass or metal, gypsum is not the best option. Nowadays, transparent or translucent epoxy, polyester, polyurethane and acrylic resins replaced materials that were used previously, as they can be colored or painted according to the artifact in restoration.

To obtain the missing parts, using a mold to pour the resin into it is the most common option. There are two ways of using molds. First is the direct method in which the mold is obtained from an area of the glass similar to the one to be reproduced. This mold is subsequently transferred to the missing area and the resin is poured directly into the mold. Second is the indirect method in which the mold is obtained from a replicated fragment. The replicated fragment is previously modeled in order to make a mold of it. Consequently, in this way the resin is poured into an indirect independent mold from the glass artifact. The method in use depends on the object, but both can damage fragile glass objects. The problem arises because sticky resins can easily slip out of the mold and stain glass. However, removing the resin without damaging the glass is complicated. In addition, another problem is the use of mold as can leave behind remains, marks, traces, and stains on the glass, so an alternative is desirable.

Testing filaments

Materials used for restoration, especially for storage and display purposes, have to pass some tests before they can be used. In this sense, these materials need to be (1) chemically stable and not prone to degradation (before or after aging) or cause degradation of the artifact after incorporation; (2) dimensionally stable, avoiding morphological changes; (3) stable in their appearance without modifications in color conditions; and (4) with a well-known chemical composition to control and prevent unwanted reactions.

In (Thickett and Lee, 2004) several tests and procedures are described to select suitable materials and ensure that they are not a source of harmful gases, so allowing them for storage or display of museum objects. An accelerated corrosion test called "3 in 1" which is based on the Oddy test has been selected to simplify the original experiment. The test consists of airtight containers which hold three metal samples near the substance that needs to be checked for its corrosive vapors. In the container, a maximum RH is maintained while the set is placed in an oven at 60 ° C for 28 days. The "3 in 1" test has been used for many years as materials that pass this test emit low levels of acetic acid, formic acid and formaldehyde vapors (Strlič*, et al.,* 2010). These elements can cause detrimental changes to artifacts that contain certain materials, so this must be analyzed in order to know if they are suitable for this purpose.

Since the last decade, conservation scientists have been researching about the effects of emissions, hence, we have a more comprehensive understanding of the degradation process in sensitive materials like ancient glass (Robinet, *et al*., 2007). Additionally, the Oddy test has been complemented or combined with instrumental analysis (Samide and Smith, 2015; Ziegler, *et al.,* 2014; Tsukada, *et al.*, 2012).

Development of analogous tests to identify morphological or color changes will be of great benefit to conservation practice. With the advancements in 3D printing materials over the past few years, there has been a remarkable increase in the use of plastic filaments by artists and recently by conservators and restorers (Shashoua, 2008). The problem arises when its composition is unknown and it emits volatile non-controlled elements or if its main properties change while degrading. Consequently, a proper test is required to check the viability of FDM filaments for restoring sensitive archaeological objects.

Document organization

This paper presents a characterization of eight different FDM filaments. Organization of the document (concerning section number 3. Results and discussion) is as follows: (i) test for determination of off-gassed pollutants emitted from printed plastic filaments, (ii) chemical characterization of the freshly and after aging printed filaments using FT-IR spectroscopy technique, (iii) optical microscopy study in the detection of morphological changes after UV radiation, (iv) identifying color and color changes of printed filaments, (v) gas chromatography-mass spectroscopy technique applied to completed characterization of printed filaments, (vi) results of application of 3D filaments in restoration of archaeological objects, and (vii) some conclusions and future research suggestions.

2. Experimental

2.1 Materials

It is crucial to clearly identify which filaments are going to be used when considering a 3D printing restoration process. In this paper, we consider filaments manufactured by "Smart materials 3D" as SMARTFIL® (Smart Materials 3D n.d.). Using filaments supplied by a registered trademark ensures control over components and absence of significant variations in composition. The selected filaments represent a small sample of the most common and easily

accessible materials on the market in order to have greater applicability and interest for professionals.

Table 1 lists all filaments studied in this research. It can be observed that acrylonitrile-butadiene-styrene (ABS) and polylactic acid (PLA) have been studied in two colors, "natural" and "white", for comparison between them. The rest of the filaments were studied in "natural" color, except for E.P., which was studied in "ivory white" as it was not supplied in the "natural" color. Filament diameters were 1.75 mm, provided on coils of 750 g, inside sealed bags with silica gel in them.

Table 1.

2.2 Methodology

1) Detection of volatile pollutants

Detection of volatile pollutants emitted from printing filament was achieved by means of the Oddy test, following the method recommended in Robinet and Thickett (2003). This test has a special importance in order to check if a potential erosion is going to appear on archaeological artifacts made of any sensitive material. In this test, oxide layers on the surfaces of the metal coupons were cleaned with a glass bristle brush and were degreased with acetone. These metal coupons were then inserted in three slots at the bottom of a silicone plug to seal the test tube after depositing freshly printed specimens in 10 x 10 x 5 mm size (figure 1). Deionized water was deposited inside a 0.8 ml tube with cotton wool on the top to avoid water condensation over metal coupons. Two series of each specimen were prepared for detection of emission of volatile pollutants and, additionally, control examinations were made without any printed specimen inside these test tubes. A Digitronic desiccation camera was used for 28 days at 60 ºC maintaining a 100% RH environment.

2) Ultraviolet (UV) radiation and FT-IR spectroscopy technique.

UV radiation has a significant impact on all organic macromolecules like polymeric materials. In order to simulate the effects of years of UV exposure under laboratory conditions and to assess if selected filaments are suitable to be used in conservation, a source of UVA-351 nm was selected to be used in a QUV-Basic (Q-Panel) accelerated aging chamber. The light source is a xenon lamp filtered to give a wavelength range from 290 to 400 nm. The test is based on standardized testing methods UNE-EN ISO 48-073-94/1 and UNE-EN ISO 4582. Specimens to be tested were printed in 76 x 22 x 1 mm size assessing chemical and color changes after 264 h to UV radiation. Samples have been analyzed by means of a FT-IR spectroscopy technique. The spectrometer used is a Vertex 70 equipment (Bruker Optics) with an attenuated total reflection system (ATR) and a room temperature DLaTGS detector. Experimental conditions were number of accumulated sweeps: 32; and resolution: 4 cm^{-1}.

3) Optical microscopy

A Leica MZ APO microscope was used to observe morphological changes on printed specimens after exposing it to UV radiation. The photon energy of radiation in the UVA and UVB range is high enough to induce damage in molecules through photochemical processes. Polymers such as macromolecules are especially affected by this as a cleavage of the polymer chain can significantly change the physical properties of the material.

4) Reflectance spectrophotometer

Color measurements of filaments, before and after accelerated UV-aging, were made with a hand-held Minolta CM-2600d spectrophotometer, 3 mm diameter aperture, set to give results in CIELAB 1976 color space. Specimens to be tested were printed in 76 x 22 x 1 mm size, testing three samples from every filament. Samples were exposed to UV radiation for 264 h. Yellowness index (YI) describes the color change occurred on a test specimen calculated by the following equation in XYZ color space:

$$YI = 100(C_X X - C_Z Z)/Y \quad (1)$$

XYZ represents International Commission Illumination (CIE) tri stimuli values using the standard 10º observer and CIE light source D65 in which C_x =1.3013; C_y =1.1498 (ASTM E313-00, 2002). To determine the total color difference between (ΔE) all three coordinates, the following formula is used:

$$\Delta E_{ab} = \sqrt{(\Delta L)^2 + (\Delta a)^2 + (\Delta b)^2} \quad (2)$$

Procedure is based on standardized testing methods UNE-EN ISO 48-073-94/1 and UNE-EN ISO 4582.

5) Gas chromatography-mas spectroscopy technique.

Chemical characterization of the substances produced by pyrolysis at different temperatures was done by gas chromatography-mass spectroscopy technique to get a completed characterization of the printed filaments. Printed specimens (less than 0.01 mg) were analyzed by direct pyrolysis Pir-GC-MS without addition of any derivatizing reagent.

The analysis was carried out on an HP-6869N gas chromatograph coupled to an HP-5973 Network selective mass detector (Hewlet-Packard, Abondale, PA, USA). The temperature of the injector was 250 °C. The chromatographic separation was performed on a capillary column of fused silica HP-5MS (30 m x 250 mm x 0.25 mm nominal). The chromatographic conditions were as follows: initial temperature of 40 °C maintained for 3 min, a ramp of 20° C/min up to 150 °C and a second ramp of 10 °C/min up to 295 °C, maintained for 10 min. The injection of the samples was carried out in split mode with a 1:20 ratio. Helium was the carrier gas used with a continuous flow velocity of 1.5 ml/min. The electronic impact was used as an ionization technique and the working conditions of the mass spectrometer were the following: temperature of the source 230 ºC, electronic energy 70 eV and scanning speed of the mass spectrometer 0.5 s/scan in the interval 20-800 m/z.

For the integration of peaks and evaluation of mass spectra, it was operated with an Agilent Chemstation G1701CA MSD software. The spectra were acquired in total ion monitoring mode and peak area data were used for the semi-quantitative analysis. The identification of the compounds was carried out by comparison with the spectra of patterns of the Wiley and NIST. The pyrolysis of the samples was carried out at 175, 230, 300, 450 and 650 ºC for 30s. A Pt (CDS Pyroprobe) spiral pre-calibrated pyrolizer was used. Both the pyrolysis chamber and the chromatographic injector were maintained at 250 °C.

6) Restoration of archaeological objects.

Original Prusa i3 MK3 3D printer from Prusa Research was used. The printer has a 0.4 mm diameter nozzle and uses 1.75 mm diameter plastic filament. Parts were printed using 0.2 mm

layer height at a 50 mm/s printing speed. An orientation of the printed part that minimized the overhangs was chosen and a support structure was enabled in the PrusaSlicer software.

3. Results and discussion

Results of the tests and instrumental analysis are presented as follows.

(i) *Test for determination of off-gassed pollutants emitted from printed plastic filaments*

The "3 in 1" test indicated that the presence of acidic volatile pollutants are not present in considerable proportions in any of the eight samples tested as visual inspection of the test coupons showed no significant changes were detected on metal coupons tested. There were three metal coupons (silver, lead and copper) and two series done for each filament tested. Figure 1 shows visual results obtained testing ABS-N. Rest of the series showed similar results.

(ii) *Chemical characterization using FT-IR spectroscopy analysis.*

Figures (2.a-7.a) show FT-IR spectra of printed plastic specimens before and after exposure to UV radiation.

FT-IR spectroscopy technique applied on samples of PLA and E.P. did not reveal appearance of new vibration bands or displacement of existing vibration bands, which suggests that no degradation has occurred in these filaments (figures 4.a- 6.a). There are only slight changes in the intensity of some vibration bands, in particular the bands at 1746 and 1042 cm^{-1}, corresponding to the tension vibrations of the C=O bond of the carbonyl group, and the tension vibrations of the C-O bonds, which suggests an increase of the terminal carboxylic groups in the polymer of PLA and E.P. indicative of the polymer chains fragmentation but without the release of lactic acid. The presence of lactic acid would result in the appearance of a broad band at 3400 cm^{-1}; a condition that is not observed.

Infrared spectra obtained for the PETG specimens before and after exposure to UV radiation did not reveal new absorption bands associated with the formation of degradation products (figure 7.a), suggesting that degradation has not occurred in this filament. Only slight changes in intensities of some absorption bands were observed in association to a polymer crystallization process. In particular, a slight increase in the intensity of the vibration bands was observed at 1471 and 1341cm^{-1}, associated with the polymer crystalline phases, but we observed different intensity on bands at 1453 and 1371cm^{-1}, corresponding to the amorphous phases.

(iii) *Optical microscopy study in the detection of morphological changes after UV radiation.*

No morphological changes on the surface of specimens have been detected by optical microscopy after exposure to UV radiation. However, PLA-W, PLA-N and E.P. Modifications commenced after 72 h UV radiation and have increased gradually with exposure. The rest of the filaments showed no variation on profiles. Visual variations on color were not observed on PLA-W, PLA-N, E.P. and PETG (figures 4.b-7.b).

(iv) Identifying color and color changes on printed filaments.

Color differences on printed filaments show that yellowing property is a noticeable consequence of UV exposure with quite remarkable increase in HIPS and ABS-N of 59.121 and 53.763, respectively, followed by ABS-W, PP and PETG with values of 18.719, 16.341, and 15.322

respectively. Rest of filaments showed no considerable changes in Yellow index (ΔYI) moving slight along yellow-blue-axis from yellow (+ b *) to blue (-b *) with negative values from 1.022 for PLA-W to 8.162 for PLA-N the lowest value of (ΔYI), (figure 10).

Filaments can be assigned into three general categories according to total color differences (ΔE*): ABS-N and HIPS greatest color degradation; PP, ABS-W and PETG intermediate color degradation; PLA-N, PLA-W, E.P. and PA minor color degradation, as total color difference (ΔE*) showed remarkable values of 34.536 and 31.845 corresponding to HIPS and ABS-N, respectively and less remarkable of 1.336 and 0.780 corresponding to E.P. and PLA-W respectively. Lightness coordinate (*L) presents slight differences in most samples with less values of 0.271 in E.P. and 0.281 in PETG. Hue angle difference (Δh°) presents the highest values in ABS-N, HIPS, PP and PETG, (table 2). Results of variations in a graph can be seen in figure 11.

Table 2.

(v) *Gas chromatography-mass spectroscopy technique applied to the complete characterization of printed filaments.*

The study by Pyrolysis GC-MS carried out with the four samples of polymers revealed a difference in its behavior. On one hand, samples PLA- N, PLA- W and E.P. (figures 12-14) exhibited a lower thermal stability, in comparison with the PETG sample (figure 15). Considering the pyrograms obtained at different temperatures for this material, in which no elements are identified in significant proportions at temperatures less than or equal to 450 ºC pyrolytic fragmentation of the polymer appears after pyrolysis at 600 °C for 30 s, including abundant toxic aromatic elements such as toluene, benzene, xylene and benzene derivatives.

Related to PLA-N, PLA-W and E.P. (tables 3-5), it can be seen that even at the lowest pyrolysis temperature (175 ºC, for 30 s), polycyclic aromatic compounds are identified, as well as lactide, which is the main decomposition product of this type of polymeric material. Results suggest that PETG (table 6) is the one that presents best thermal stability.

Table 3-6

(vi) R*esults of application of 3D filaments in restoration of archaeological objects.*

Four replicated bowls (figure 16) were produced for assessing the 3D filament behavior restoration of archaeological objects. Filaments used were those with a higher UV radiation stability in the FT-IR study and less color changes from reflectance spectrophotometer study (figures 4.b-7.b). No significant differences were observed between the four printed replicas on PLA-W, PLA-N, E.P. and PETG, neither in their form nor in their volume. Total print time for each replicated model was estimated in 5 h and 20 min with an infill density of 20%.

Same printing conditions were used for restoration of a sensitive archaeological glass bowl from the collection of Manises Ceramic Museum (Valencia, Spain), manufactured by glassblowing and dated from the 17th century (figure 17). The estimated printing was two hours and restoration was done with PLA-W.

Rapid prototyping using FDM is appropriate for restoring sensitive archaeological objects, allowing reconstruction of parts and decreasing risk while manipulating delicate artifacts.

(vii) *Some conclusions and future research suggestions.*

Eight polymeric materials used in FDM have been tested and classified as suitable to be applied for restoration of sensitive archaeological objects.

The results obtained give an insight about the degradation caused in the filaments after exposure to UV radiation. Hence, this exhibits the viability of using materials for conservation treatments for artifacts kept in the museum environment. A hand-made ceramic bowl was replicated in PLA-N, PLA-W, E.P. and PETG to study behavior and differences in filaments.

Finally, the restoration of a fragile and sensitive glass artifact was performed using PLA-W filament. This is a non-invasive method which offers an alternative treatment, so restoration is performed taking into account polycyclic aromatic compounds identified in PLA-W filament at pyrolysis temperature (175 ºC). To avoid any interference between elements released at print temperature (200±20 ºC) from the filament, printed parts remained for 90 days without being incorporated to the artifact until volatile pollutants completely disappeared. The result is comparable to that obtained by traditional restoration methods, but it preserves and safeguards the fragile glass artifact because of its minimum manipulation.

In further research steps, a greater number of 3D filaments can be analyzed, together with the development of a method to setup and apply paints and prepare layers to imitate ancient opacified deteriorated glass.

Acknowledgements

This work is supported by the Spanish Ministry of Economy, Industry and Competitiveness and the European Regional Development Fund (ERDF), in the context of the research project *"Desarrollo de un Sistema Integrado de Restauración, Recomposición, Restitución y Representación de Fragmentos Arqueológicos":* HAR2015-69408-R (MINECO-FEDER).

Authors want to express their gratitude to Mr. Antonio Doménech from the Universitat de València for Chemical characterization using FT-IR spectroscopy and gas chromatography spectroscopy techniques. Authors would also like to acknowledge the collaboration of the Manises Ceramic Museum for their support to this paper, providing access to restored archaeological artifacts.

We want to thank Editage (www.editage.com) for the English edition.

References

Alemanno, G. et al., 2014. Interlocking Pieces for Printing Tangible Cultural Heritage Replicas. In: *Eurographics Workshop on Graphics and Cultural Heritage (2014).* s.l.: Reinhard Klein and Pedro Santos.

Balletti, C., Ballarin, M. & Guerra, F., 2017. 3D printing: State of the art and future perspectives. *Journal of Cultural Heritage,* 9 March, Volume 26, pp. 172-182.

Behzadnasab, M., Yousefi, A., Ebrahimibagha, D. & Nasiri, F., 2019. Effects of processing conditions on mechanical properties of PLA printed parts. Rapid prototyping Journal, 26, pp. 381-389.

Cantrell, J. et al., 2016. Experimental characterization of the mechanical properties of 3D-printed ABS and polycarbonate parts. *Rapid Prototyping Journal,* 23(4), pp. 811-824.

Grasso, M. et al., 2018. Effect of temperature on the mechanical properties of 3D-printed PLA tensile specimens. *Rapid Prototyping Journal,* 24(8), pp. 1337-1346.

Robinet, L. & Thickett, D., 2003. A New Methodology for Accelerated Corrosion Testing. *Studies in Conservation,* 48(4), pp. 263-268.

Robinet, L. et al., 2007. Effect of organic acid vapours on the alteration of soda silicate glass. *Journal of non-crystalline solids,* Issue 353, pp. 1546-1559.

Samide, M. J. & Smith, G. D., 2015. Analysis and quantitation of volatile organic compounds emitted from plastics used in museum construction by evolved gas analysis-gas chromatography-mass spectrometry. *Journal of Chromatography A,* pp. 201-208.

Schwartz, J. et al., 2020. Not all PLA filaments are created equal: an experimental investigation. *Rapid Prototyping Journal,* 26(7), pp. 1263-1276.

Scopigno, R. et al., 2014. Digital Fabrication Technologies for Cultural Heritage. In: *Eurographics Workshop on Graphics and Cultural Heritage (2014).* s.l.:s.n.

Seixas, M. et al., 2016. The use of rapid prototyping in the joining of fractured historical silver objects. *Rapid Prototyping Journal,* 24(3), pp. 532-538.

Shashoua, Y., 2008. *Conservation of plastics: Materials science, degradation and preservation.* Oxford: Butterworth-Heinemann.

Smart Materials 3D, n.d. *Smart Materials 3D, products*. [Online] Available at: http://smartmaterials3d.com/en/15-products [Accessed 11 August 2020].

Soares, J. et al., 2018. Analysis of the influence of polylactic acid (PLA) colour on FDM 3D printing temperature and part finishing. *Rapid Prototyping Journal,* 24(8), pp. 1305-1316.

Strlič, M. et al., 2010. Test for compatibility with organic heritage materials. A proposed procedure. *e-Preservation Science,* Issue 7, pp. 78-86.

Thickett, D. & Lee, L. R., 2004. Selection of Materials for the Storage or Display of Museum Objects. *The British Museum Occasional Paper,* Issue Number 111, pp. 1-30.

Tsukada, M., Rizzo, A. & Granzotto, C., 2012. A New Strategy for Assessing Off-Gassing from Museum Materials: Air Sampling in Oddy Test Vessels. *AIC NEWS,* January, 37(1), pp. 1-7.

Tucci, G., Bonora, V., Conti,. A. & Fiorini, L., 2017. HIGH-QUALITY 3D MODELS AND THEIR USE. In: *The International Archives of the Photogrammetry, Remote Sensing and Spatial Information Sciences.* Ottawa (Canada): 26th International CIPA Symposium 2017, pp. 687-693.

Vatani, M. & Choi, J., 2015. Direct-print photopolymerization for 3D printing. *Rapid Prototyping Journal,* 23(2), pp. 337-343.

Yang, M., Lv, X.-g. & Zhang, J., 2018. Research on colour 3D printing based on colour adherence. *Rapid Prototyping Journal,* 24(1), pp. 37-45.

Zang, F., Campell, R. I. & Graham, I. J., 2015. Application of Additive Manufacturing to the Digital Restoration of Archaeological Artifacts. *Procedia Technology,* Volume 20, pp. 249-257.

Ziegler, J., Khun-Wawrzinek, C., Eska, M. & Eggert, G., 2014. *Popping Stoppers, Crumbling Coupons - Oddy Testing of Common Cellulose Nitrate Ceramic Adhesives.* Melbourne, Paris: International Council of Museums, pp. art. 0505, 8 pp.

UNE-EN ISO 48-073-94/1 Paints and Varnishes. Colorimetry. Part 1: Principles

UNE-EN ISO 4582 Plastics. Determination of changes in colour and variations in properties after exposure to daylight under the glass, natural weathering or laboratory light sources.

LIST OF FIGURES

Figure 12. Pyrogram obtained from PLA-N.

Figure 13. Pyrogram obtained from PLA-W.

Figure 14. Pyrogram obtained from E.P.

Figure 15. Pyrogram obtained from PETG.

Figure 16. A ceramic hand-made bowl replicated four times with E.P., PLA-W, PLA-N and PETG filaments. First line shows interior views and second line shows lateral views. No significant differences were observed between the four replicas, neither in their form nor in their volume.

Figure 17. Rapid prototyping using FDM was applied for restoration of fragile and sensitive archaeological glass bowl using PLA-W filament testing: (a) frontal, (b) bottom, (c) right, (d) back, (e) top and (f) left views.

Table 1. Filaments studied.

Table 2. SCI differences after the exposure to the UV radiation of lightness (ΔL*), chroma (ΔC*), tone (Δhº), total color variation (ΔE*ab), and yellowness (ΔYI) values.

Table 3. Compounds identified in PLA-N sample analysed by the gas chromatography-mass spectroscopy technique.

Table 4. Compounds identified in PLA-W sample analysed by the gas chromatography-mass spectroscopy technique.

Table 5. Compounds identified in E.P. sample analysed by the gas chromatography spectroscopy-mass technique.

Table 6. Compounds identified in PETG sample analysed by the gas chromatography-mass spectroscopy technique.

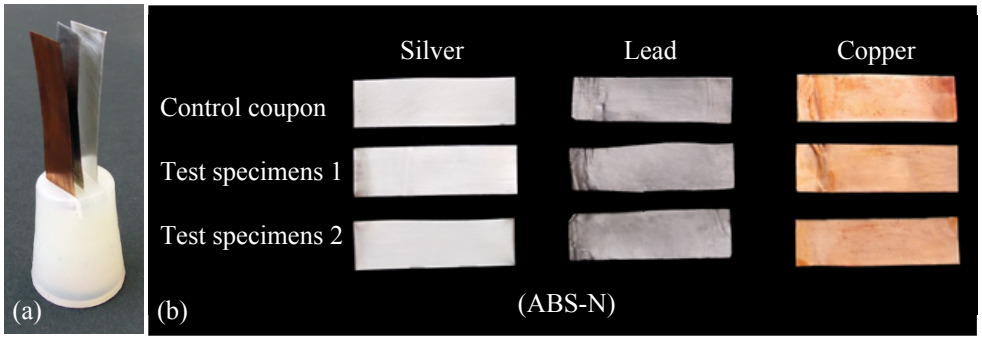
Silver
Lead
Copper
Control coupon
Test specimens 1
Test specimens 2
(a)
(b)
(ABS-N)

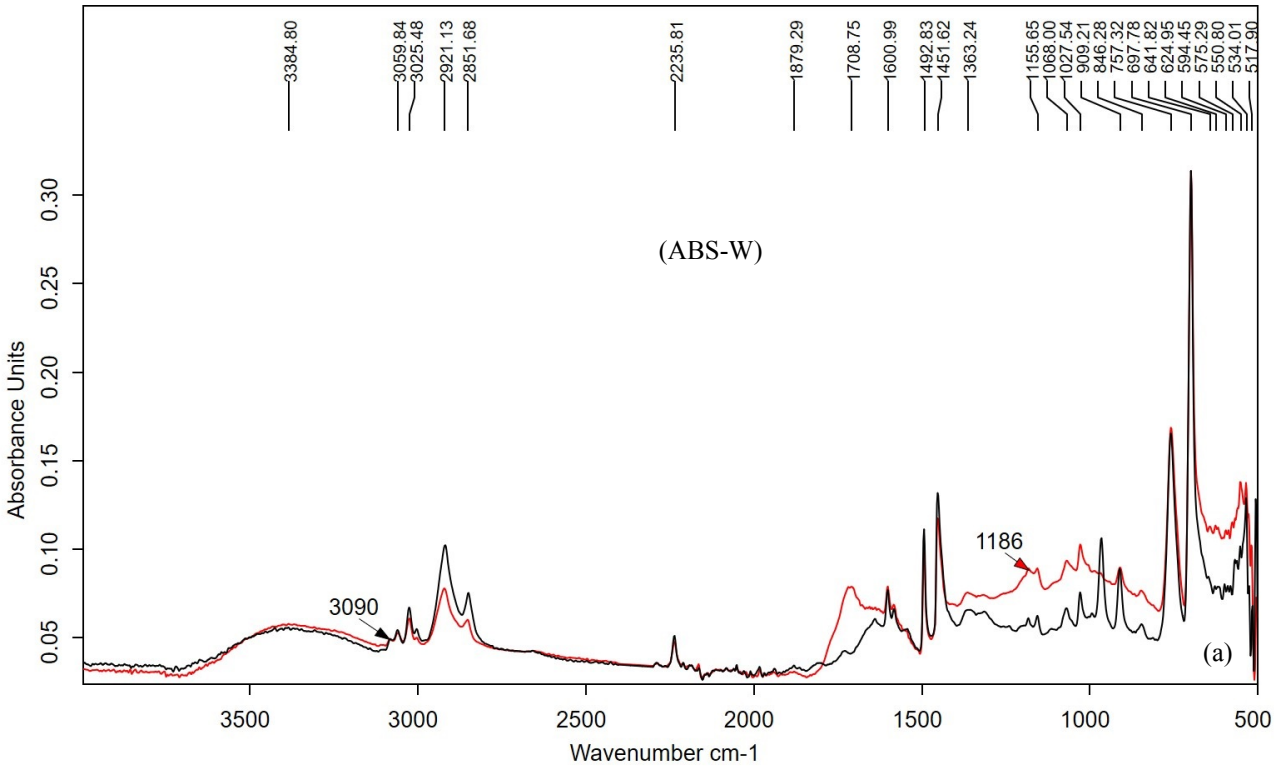
3384.80
3059.84
3025.48
2921.13
2851.68
2235.81
1879.29
1708.75
1600.99
1492.83
1451.62
1363.24
1155.65
1068.00
1027.54
909.21
846.28
757.32
697.78
641.82
624.95
594.45
575.29
550.80
534.01
517.90
(ABS-W)
Absorbance Units
0.05
0.10
0.15
0.20
0.25
0.30
3090
1186
(a)
3500
3000
2500
2000
1500
1000
500
Wavenumber cm-1


0h
264h
(b)

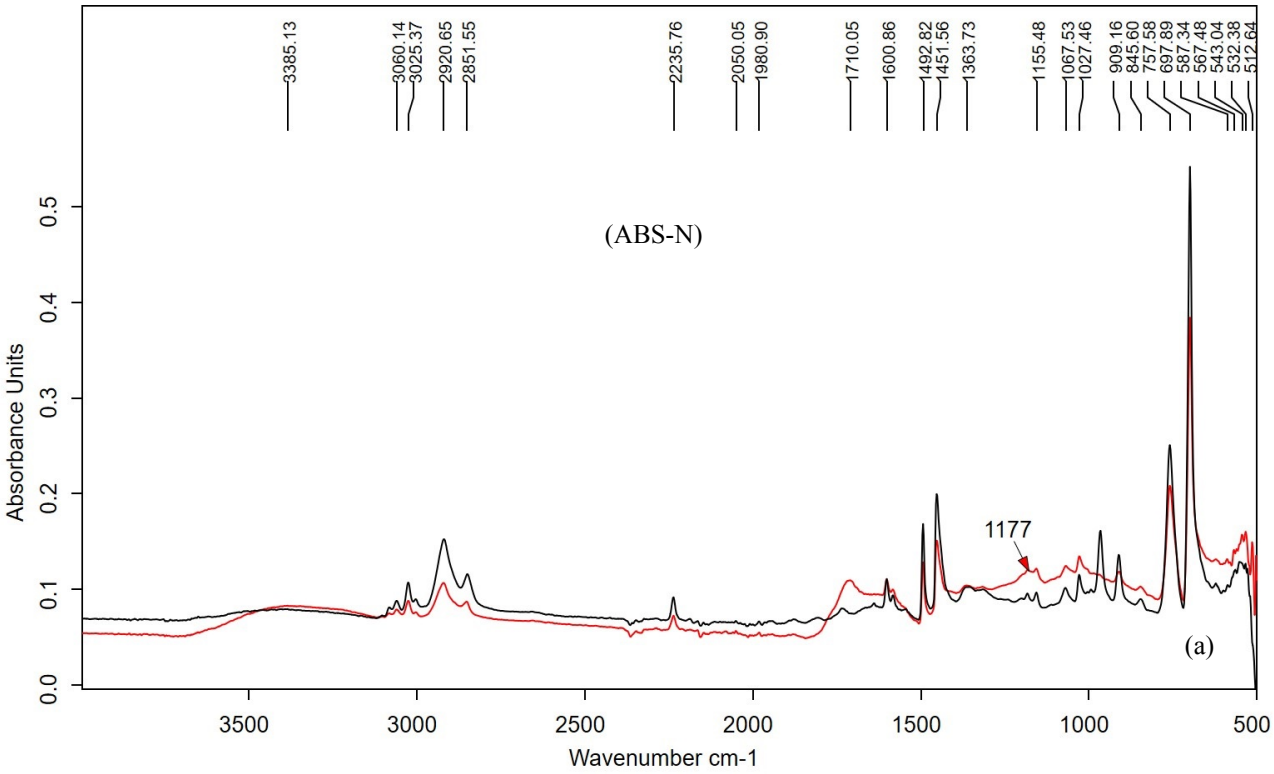
3385.13
3060.14
3025.37
2920.65
2851.55
2235.76
2050.05
1980.90
1710.05
1600.86
1492.82
1451.56
1363.73
1155.48
1067.53
1027.46
909.16
845.60
757.58
697.89
587.34
567.48
543.04
532.38
512.64
(ABS-N)
1177
(a)
Absorbance Units
0.0
0.1
0.2
0.3
0.4
0.5
3500
3000
2500
2000
1500
1000
500
Wavenumber cm-1


0h
264h
(b)

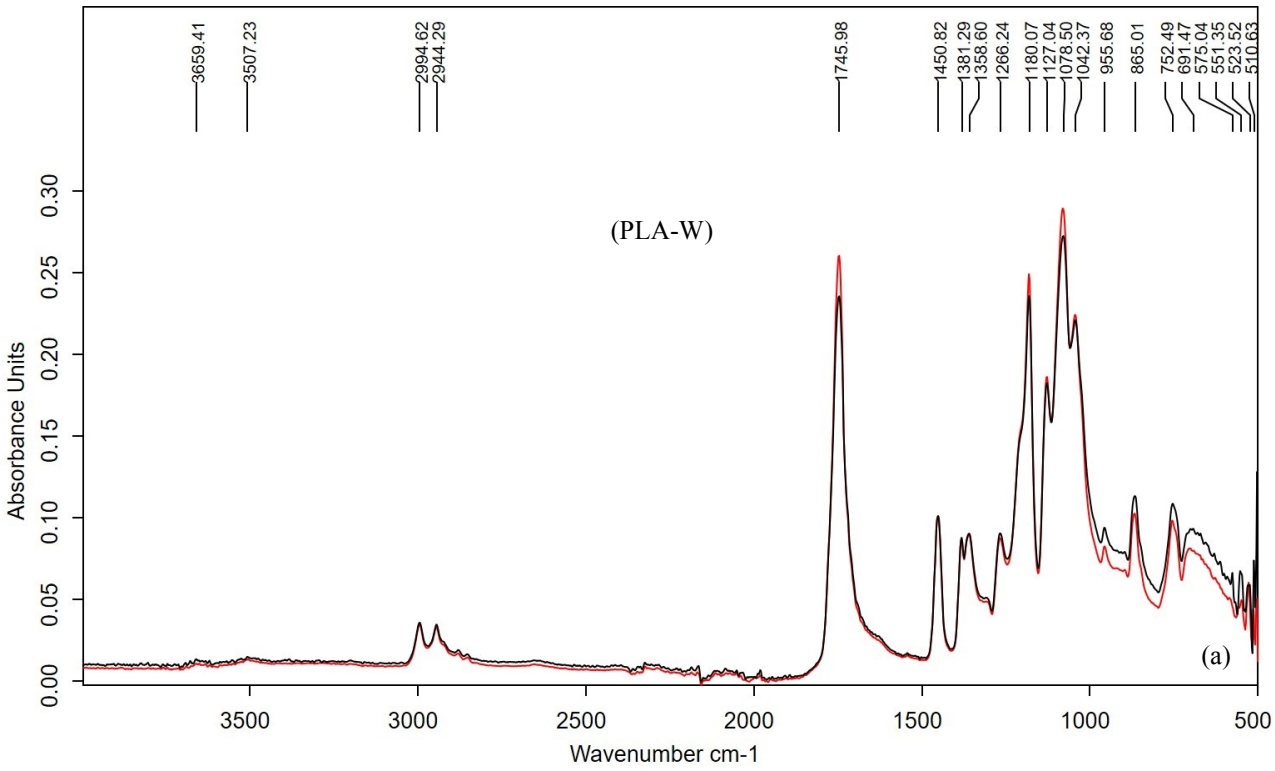
3659.41
3507.23
2994.62
2944.29
1745.98
1450.82
1381.29
1358.60
1266.24
1180.07
1127.04
1078.50
1042.37
955.68
865.01
752.49
691.47
575.04
551.35
523.52
510.63
(PLA-W)
Absorbance Units
0.00
0.05
0.10
0.15
0.20
0.25
0.30
3500
3000
2500
2000
1500
1000
500
Wavenumber cm-1
(a)


0h
264h
(b)

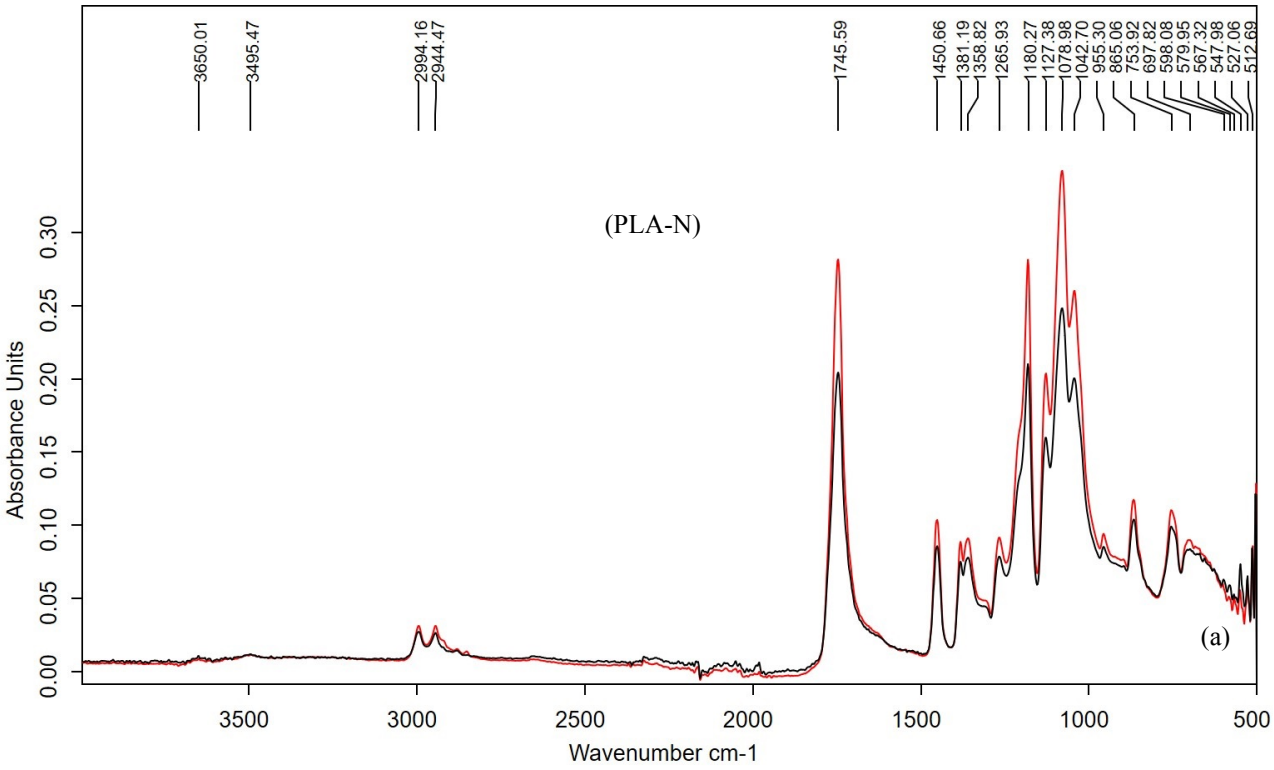
3650.01
3495.47
2994.16
2944.47
1745.59
1450.66
1381.19
1358.82
1265.93
1180.27
1127.38
1078.98
1042.70
955.30
865.06
753.92
697.82
598.08
579.95
567.32
547.98
527.06
512.69
(PLA-N)
Absorbance Units
0.00
0.05
0.10
0.15
0.20
0.25
0.30
3500
3000
2500
2000
1500
1000
500
Wavenumber cm-1
(a)

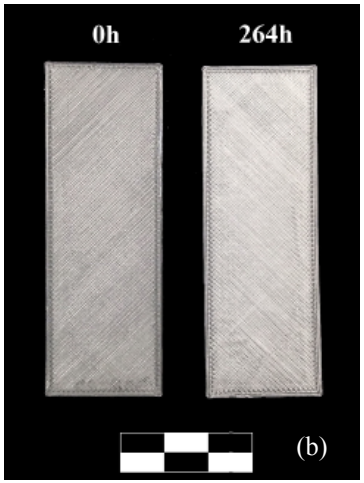
0h
264h
(b)

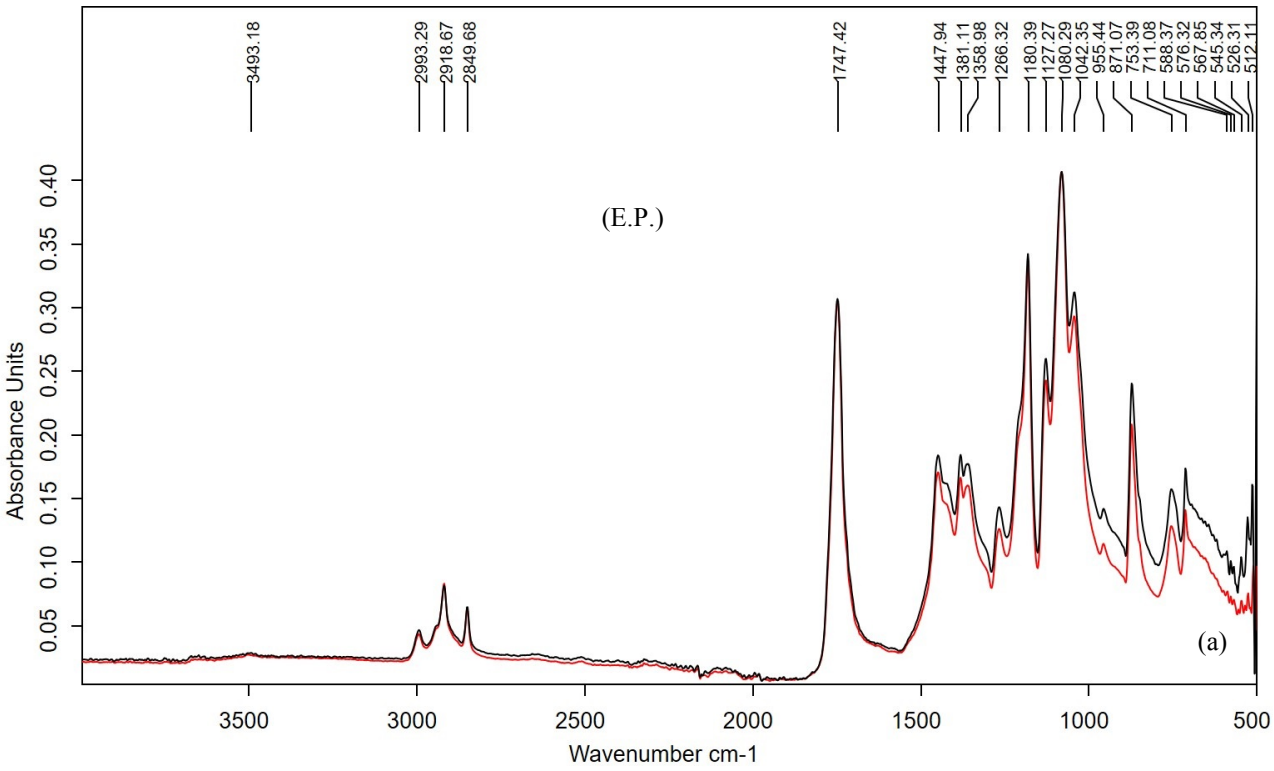
3493.18
2993.29
2918.67
2849.68
1747.42
1447.94
1381.11
1358.98
1266.32
1180.39
1127.27
1080.29
1042.35
955.44
871.07
753.39
711.08
588.37
576.32
567.85
545.34
526.31
512.11
(E.P.)
Absorbance Units
0.05
0.10
0.15
0.20
0.25
0.30
0.35
0.40
(a)
3500
3000
2500
2000
1500
1000
500
Wavenumber cm-1


0h
264h
(b)

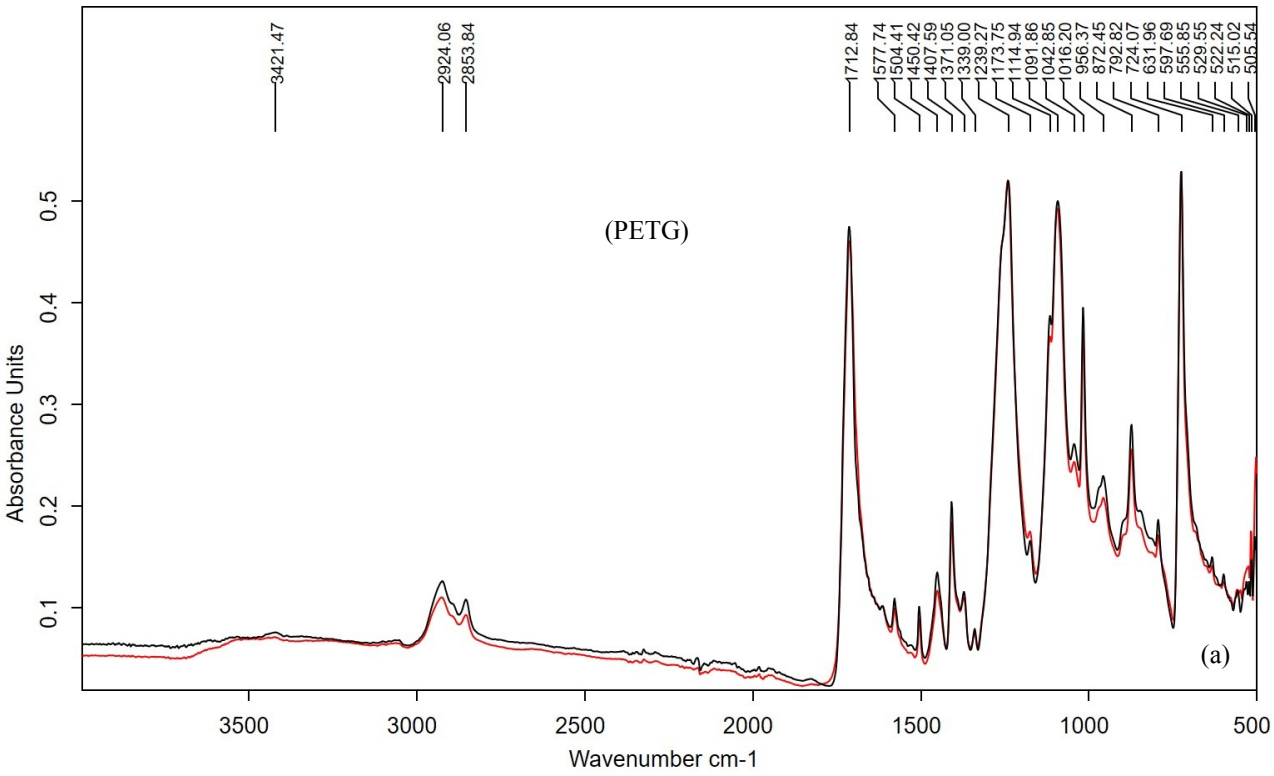
3421.47
2924.06
2853.84
1712.84
1577.74
1504.41
1450.42
1407.59
1371.05
1339.00
1239.27
1173.75
1114.94
1091.86
1042.85
1016.20
956.37
872.45
792.82
724.07
631.96
597.69
555.85
529.55
522.24
515.02
505.54
(PETG)
Absorbance Units
0.1
0.2
0.3
0.4
0.5
3500
3000
2500
2000
1500
1000
500
Wavenumber cm-1
(a)


0h
264h
(b)

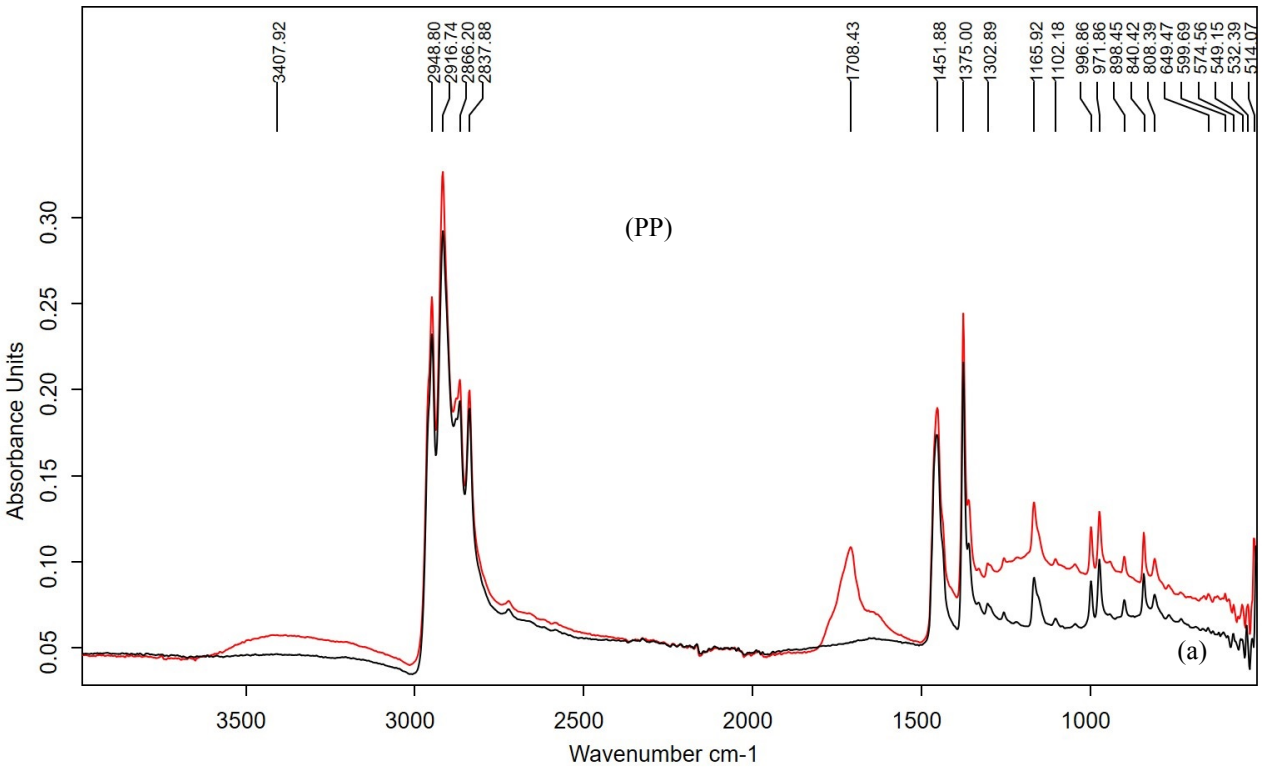
3407.92
2948.80
2916.74
2866.20
2837.88
1708.43
1451.88
1375.00
1302.89
1165.92
1102.18
996.86
971.86
898.45
840.42
808.39
649.47
599.69
574.56
549.15
532.39
514.07
(PP)
Absorbance Units
0.05
0.10
0.15
0.20
0.25
0.30
3500
3000
2500
2000
1500
1000
Wavenumber cm-1
(a)

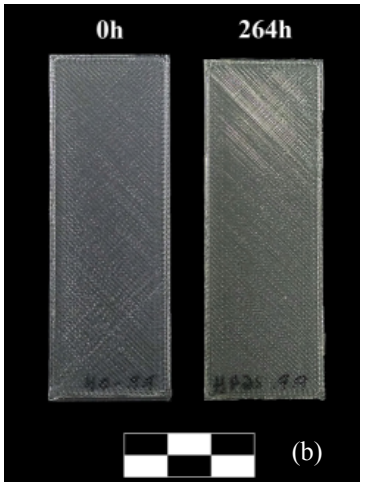
0h
264h
(b)

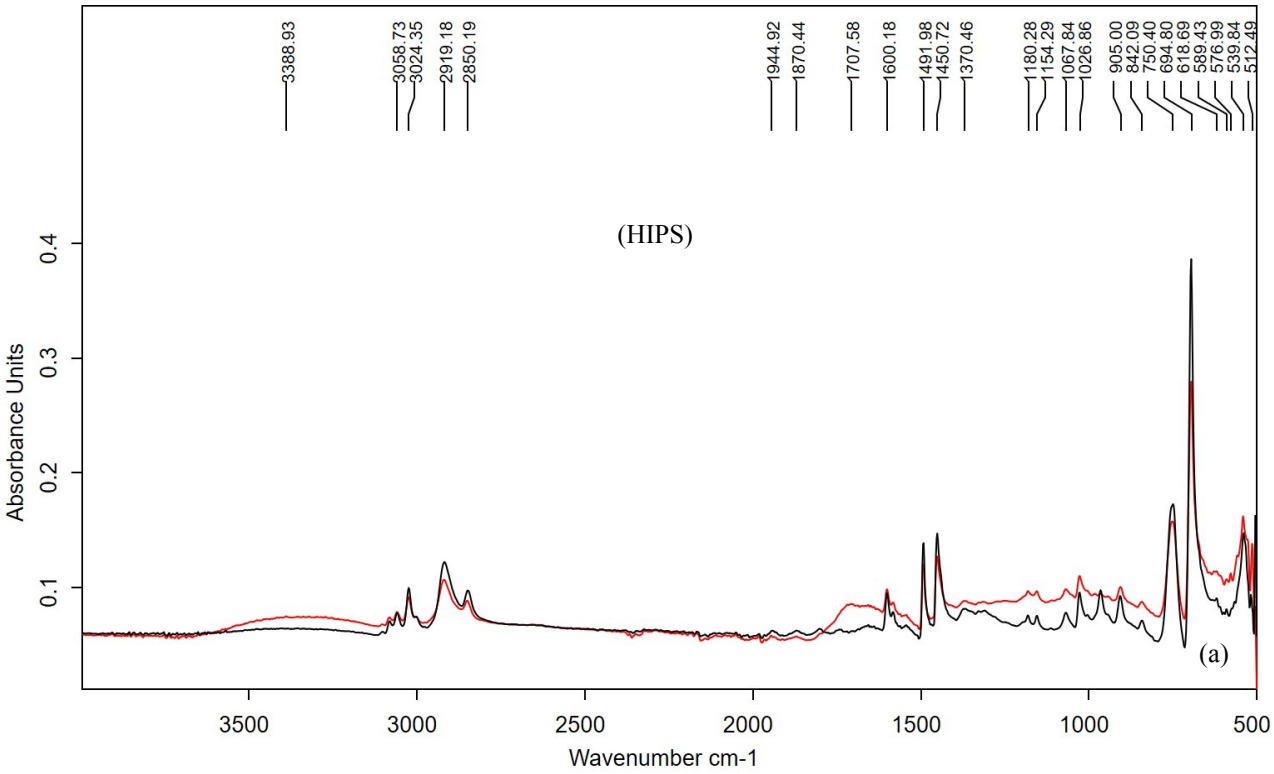
3388.93
3058.73
3024.35
2919.18
2850.19
1944.92
1870.44
1707.58
1600.18
1491.98
1450.72
1370.46
1180.28
1154.29
1067.84
1026.86
905.00
842.09
750.40
694.80
618.69
589.43
576.99
539.84
512.49
(HIPS)
Absorbance Units
0.1
0.2
0.3
0.4
(a)
3500
3000
2500
2000
1500
1000
500
Wavenumber cm-1

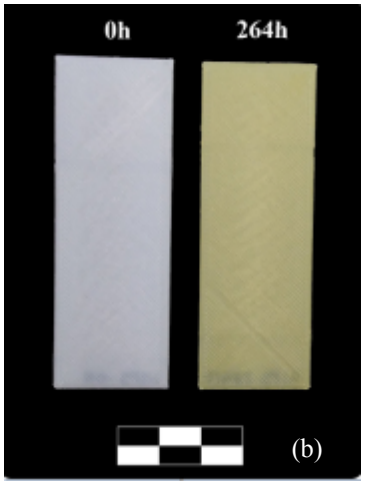
0h
264h
(b)

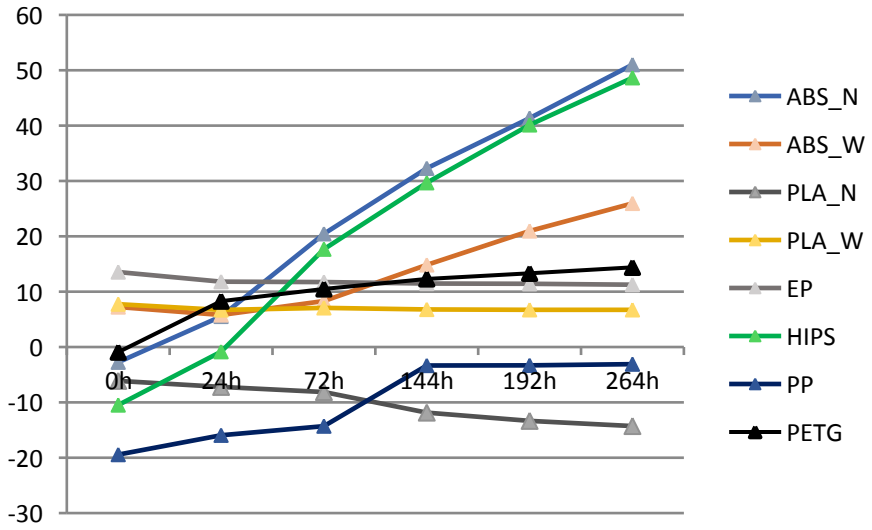
60
50
40
30
20
10
0
-10
-20
-30
0h
24h
72h
144h
192h
264h
ABS_N
ABS_W
PLA_N
PLA_W
EP
HIPS
PP
PETG

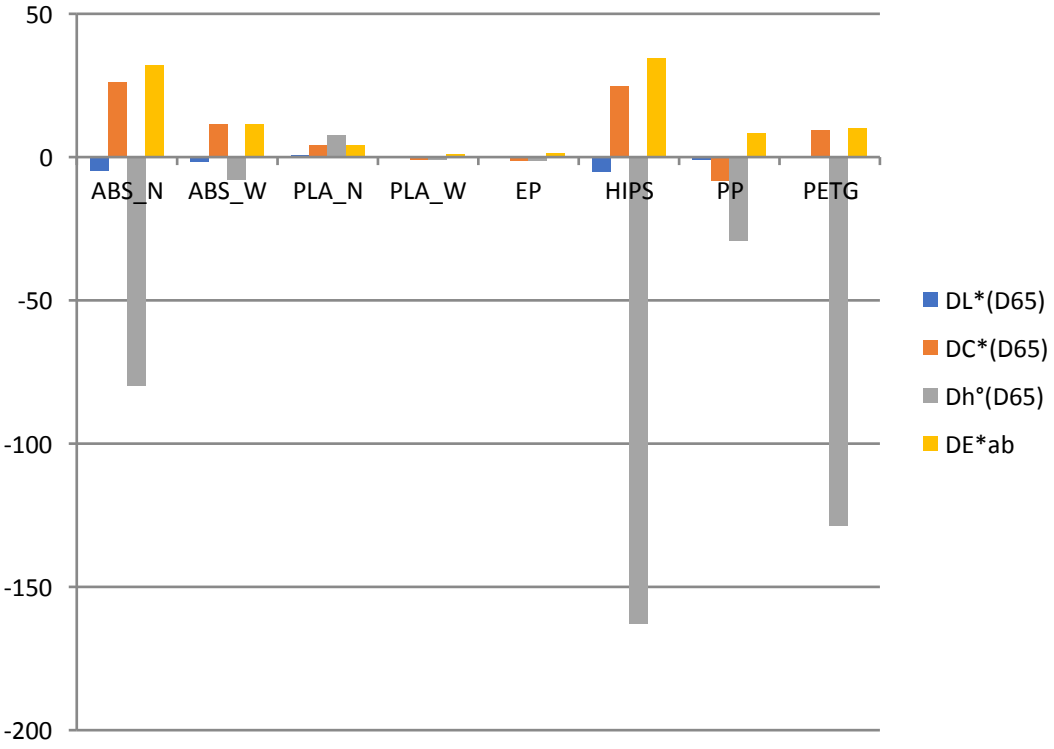
50
0
-50
-100
-150
-200
ABS_N
ABS_W
PLA_N
PLA_W
EP
HIPS
PP
PETG
DL*(D65)
DC*(D65)
Dh°(D65)
DE*ab

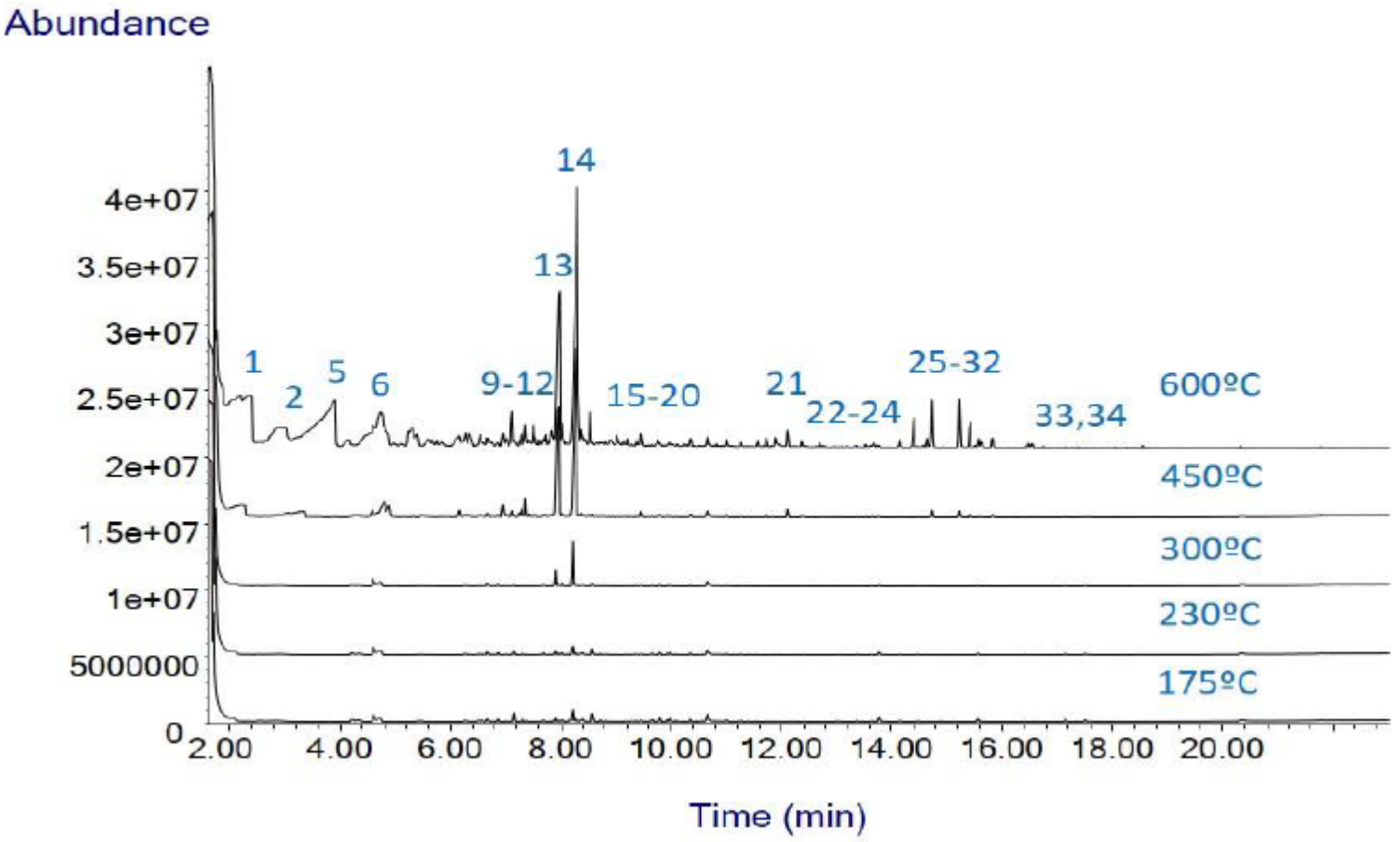
Abundance
4e+07
3.5e+07
3e+07
2.5e+07
2e+07
1.5e+07
1e+07
5000000
0
1
2
5
6
9-12
13
14
15-20
21
22-24
25-32
33,34
600ºC
450ºC
300ºC
230ºC
175ºC
2.00
4.00
6.00
8.00
10.00
12.00
14.00
16.00
18.00
20.00
Time (min)

(PLA-N)

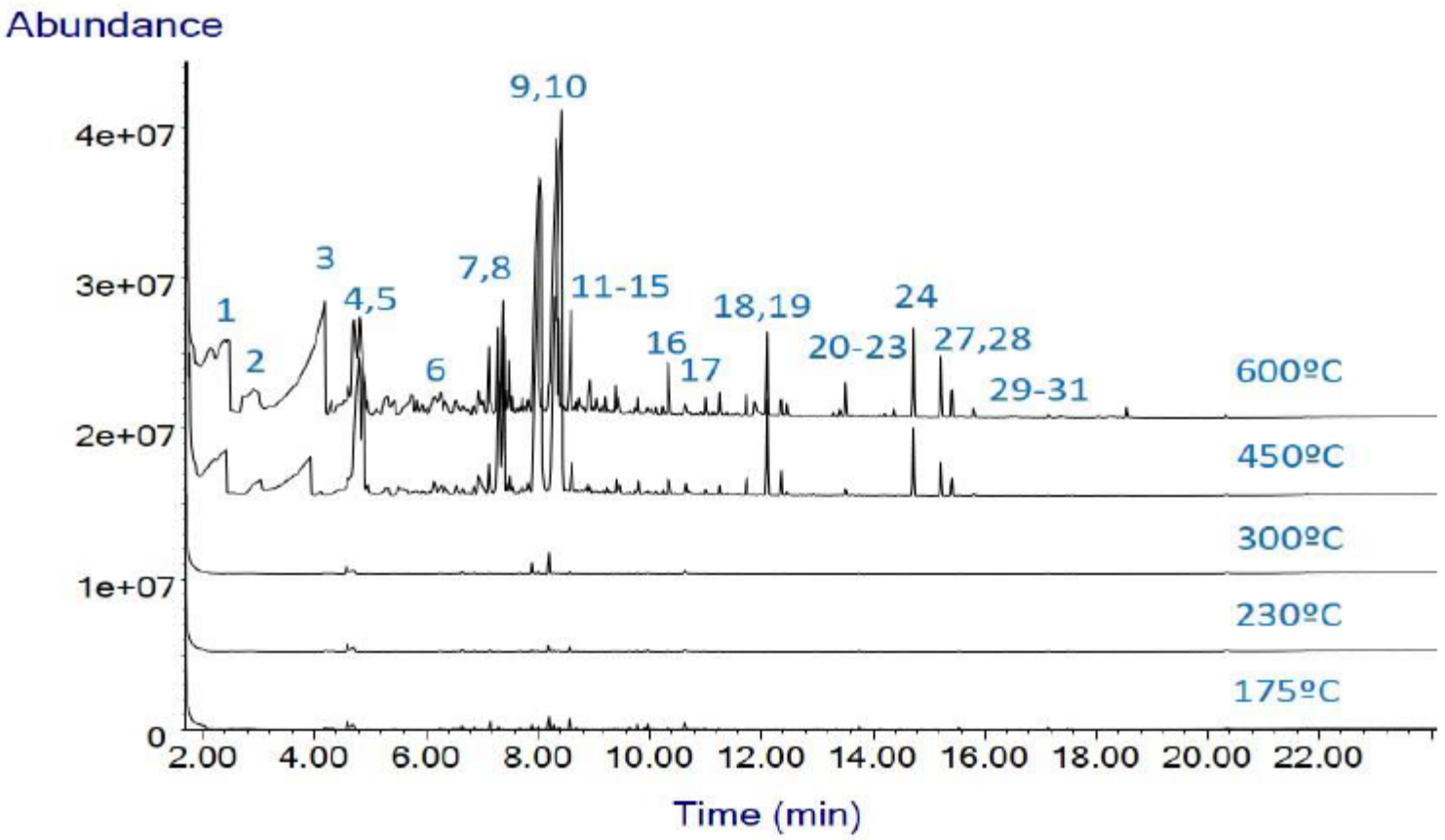
Abundance
4e+07
3e+07
2e+07
1e+07
0
1
2
3
4,5
6
7,8
9,10
11-15
16
17
18,19
20-23
24
27,28
29-31
600ºC
450ºC
300ºC
230ºC
175ºC
2.00
4.00
6.00
8.00
10.00
12.00
14.00
16.00
18.00
20.00
22.00
Time (min)

(PLA-W)

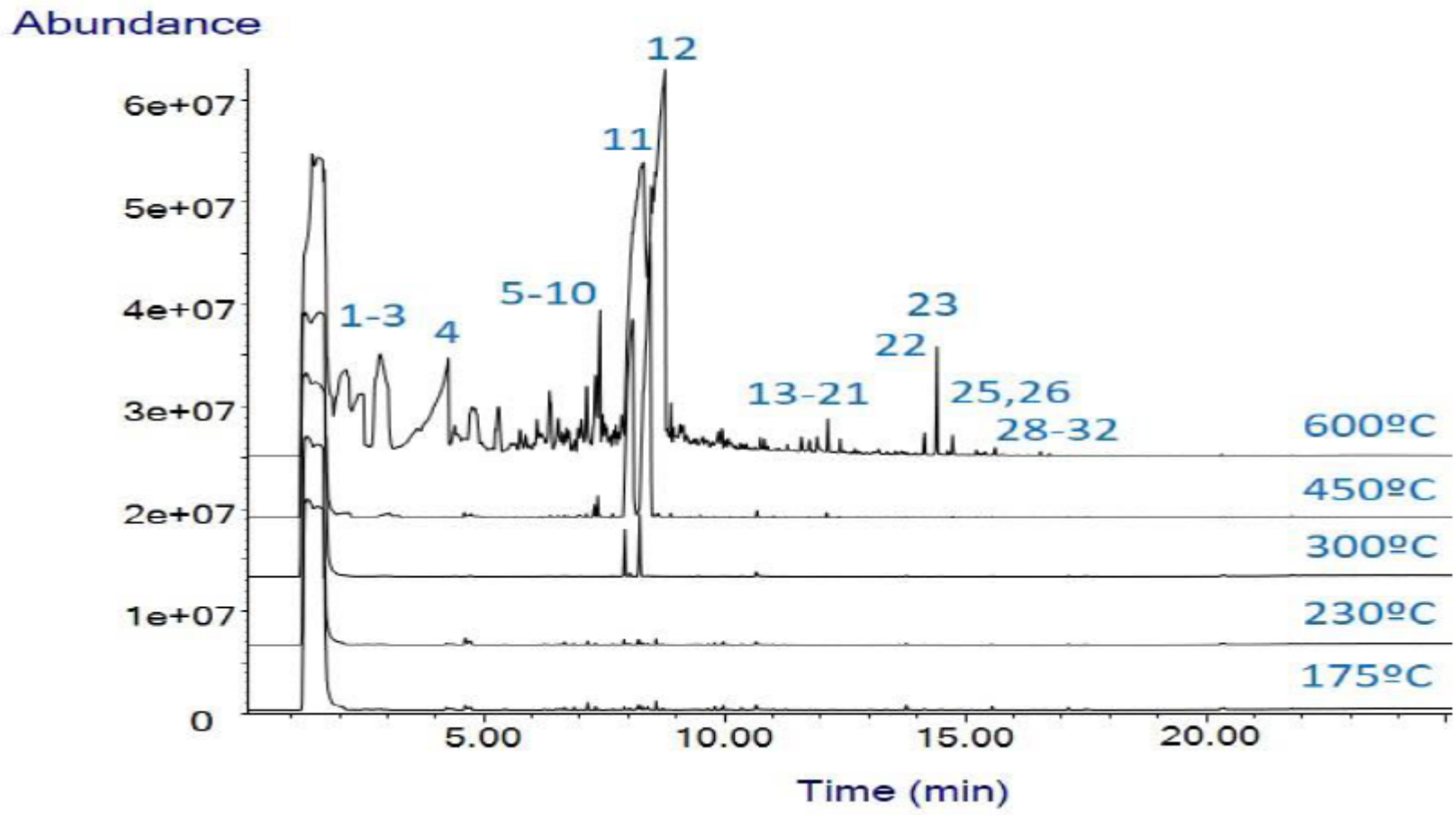
Abundance
6e+07
5e+07
4e+07
3e+07
2e+07
1e+07
0
1-3
4
5-10
11
12
13-21
22
23
25,26
28-32
600ºC
450ºC
300ºC
230ºC
175ºC
5.00
10.00
15.00
20.00
Time (min)

(E.P.)

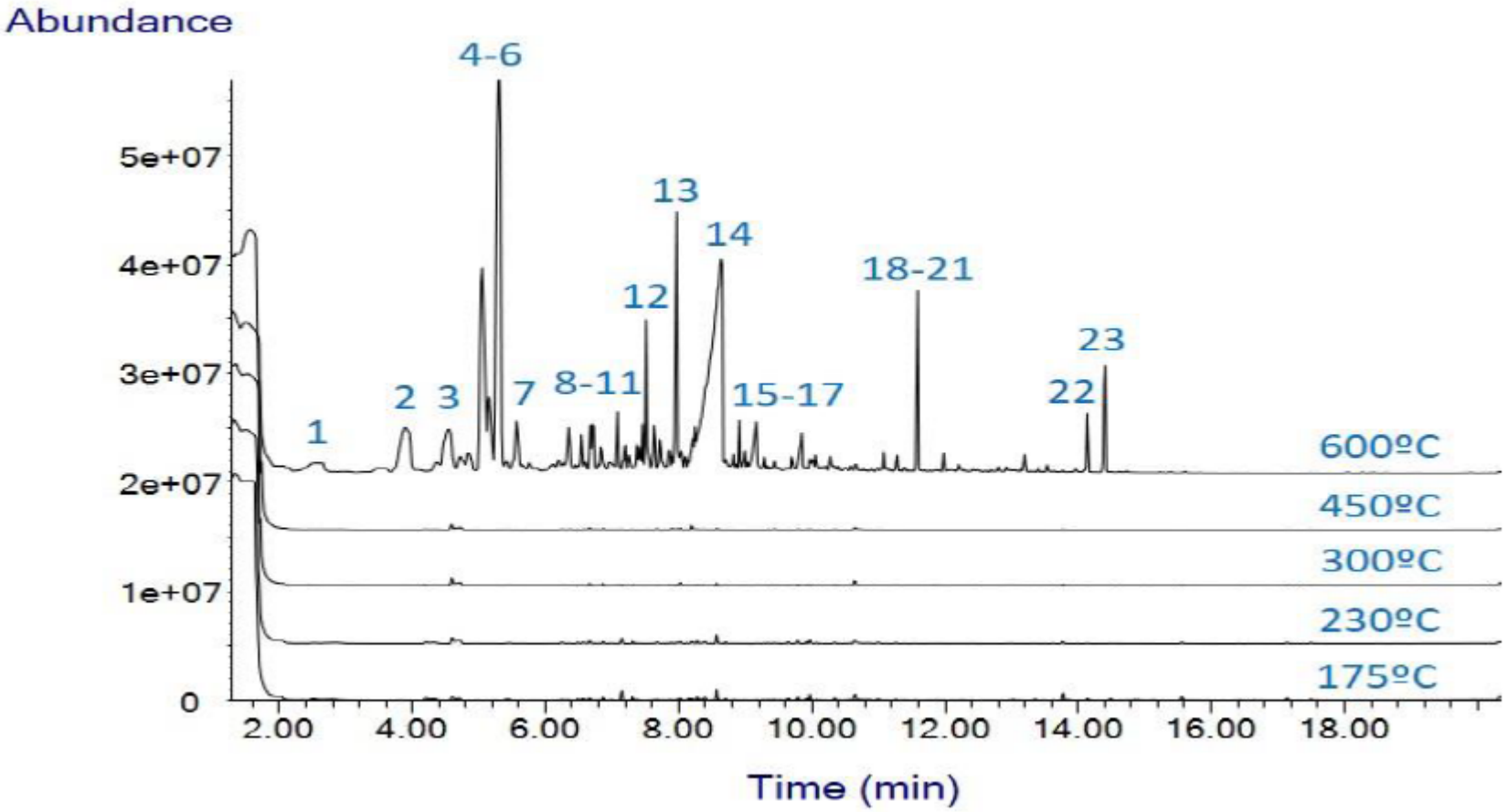
Abundance
4-6
13
14
18-21
12
23
2 3
7
8-11
15-17
22
1
600ºC
450ºC
300ºC
230ºC
175ºC
5e+07
4e+07
3e+07
2e+07
1e+07
0
2.00
4.00
6.00
8.00
10.00
12.00
14.00
16.00
18.00
Time (min)

(PETG)

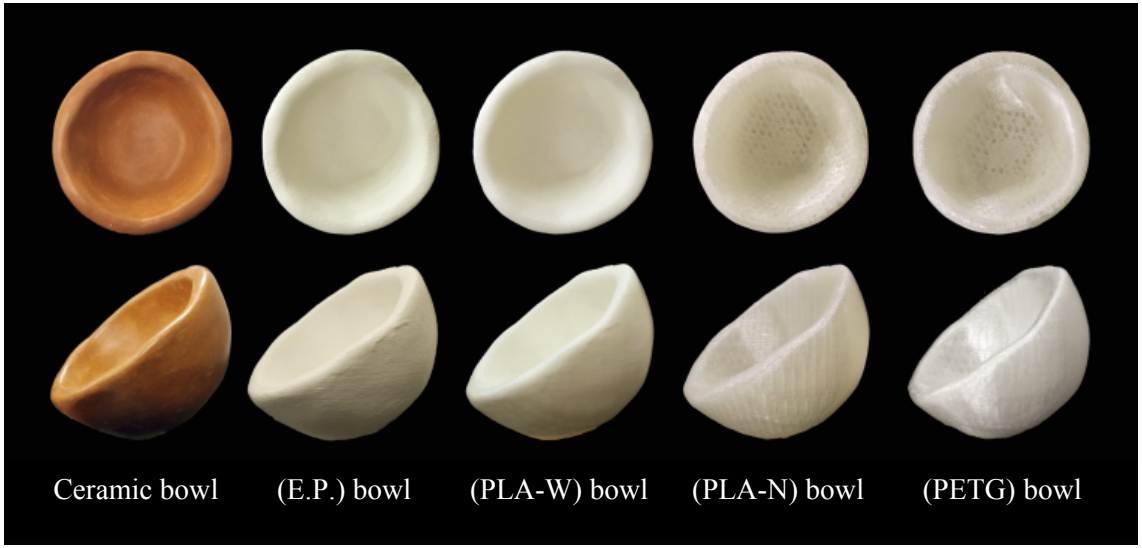
Ceramic bowl
(E.P.) bowl
(PLA-W) bowl
(PLA-N) bowl
(PETG) bowl

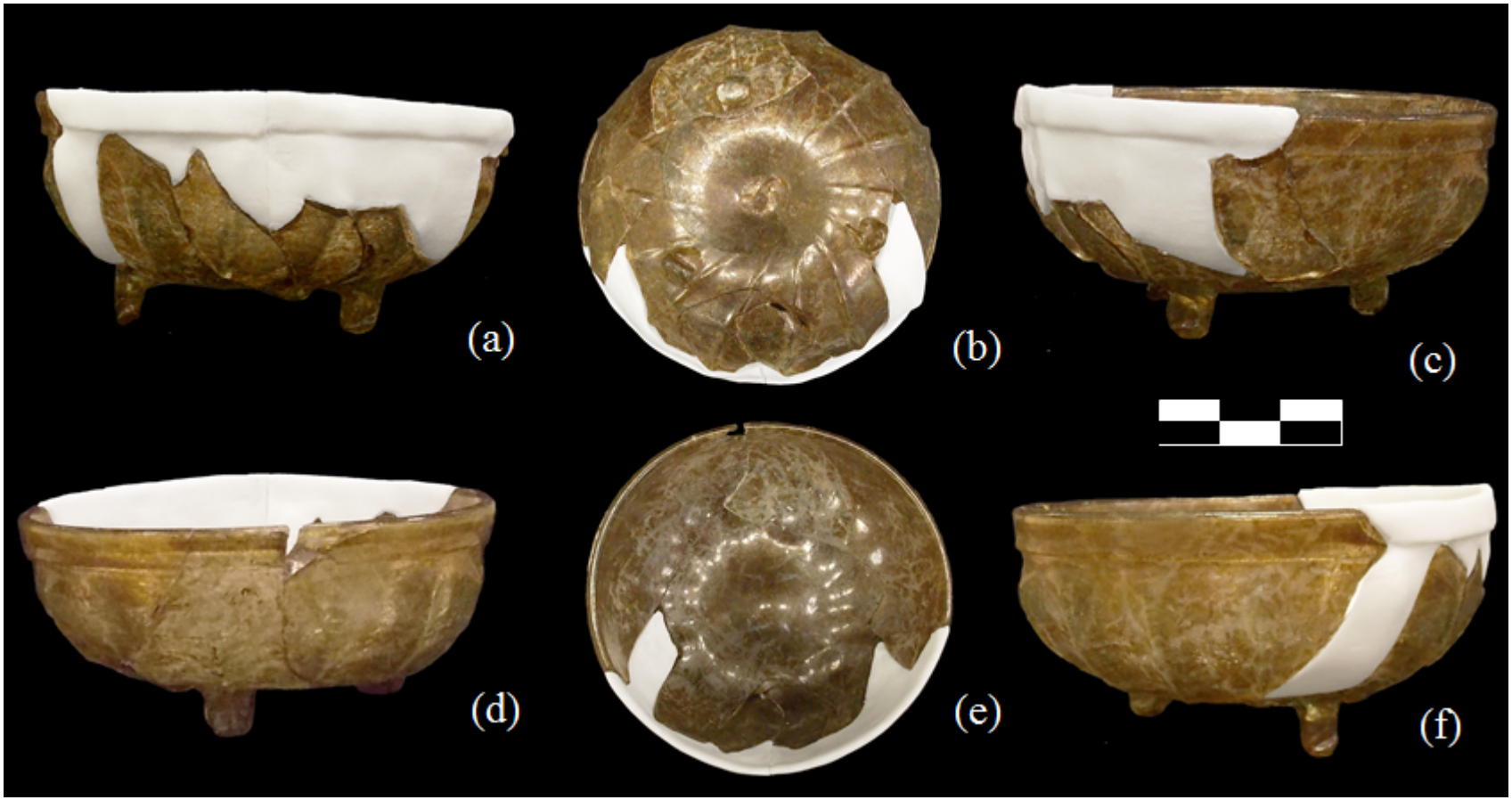
(a)
(b)
(c)
(d)
(e)
(f)

Chemical name	Name color	Abbreviation	Print temperature (ºC)	Hot pad (ºC)	Name product
acrylonitrile-butadiene-styrene	Ivory white	(ABS-W)	240±10 ºC	80-100 ºC	SMARTFIL®ABS
acrylonitrile-butadiene-styrene	Natural	(ABS-N)	240±10 ºC	80-100 ºC	SMARTFIL®ABS
polylactic acid	Ivory white	(PLA-W)	220±20 ºC	0-60 ºC	SMARTFIL®PLA
polylactic acid	Natural	(PLA-N)	220±20 ºC	0-60 ºC	SMARTFIL®PLA
polylactide acid with $CaCO_3$	Ivory white	(E.P.)	200±10 ºC	0-60 ºC	SMARTFIL®E.P.
polyethylene terephtalate glycol	Natural	(PETG)	235±10 ºC	60-90 ºC	SMARTFIL®PETG
polypropylene	Natural	(PP)	220±10 ºC	60-100 ºC	SMARTFIL®PP
high impact polystyrene	Natural	(HIPS)	235±10 ºC	80-100 ºC	SMARTFIL®HIPS

		ΔL*(D65)	ΔC*(D65)	Δh°(D65)	ΔE*ab	ΔYI
ABS_N	x	-4,603	25,934	-79,677	31,845	53,763
	δ	-0,202	-2,355	-86,627	5,947	-4,322
ABS_W	x	-1,569	11,323	-7,778	11,488	18,719
	δ	0,122	0,063	-0,521	0,135	0,070
PLA_N	x	0,424	4,076	7,738	4,140	-8,162
	δ	0,228	0,091	-0,120	0,247	0,085
PLA_W	x	-0,283	-0,723	-1,007	0,780	-1,022
	δ	0,239	0,037	0,219	0,242	0,008
EP	x	0,271	-1,300	-1,278	1,336	-2,286
	δ	0,066	0,027	-0,012	0,071	0,035
HIPS	x	-5,132	24,684	-162,719	34,536	59,121
	δ	0,008	0,190	-0,169	0,196	-0,064
PP	x	-0,960	-8,073	-29,002	8,315	16,341
	δ	0,120	0,092	5,506	0,174	0,080
PETG	x	0,281	9,202	-128,711	9,877	15,322
	δ	-0,102	0,065	-10,001	0,117	0,034

PLA-N							
Peak	T_R	Compound	175ºC	230ºC	300ºC	450ºC	600ºC
1	2,44	Acetic Acid				√	√
2	2,85	2,3-Pentanedione					√
3	3,06	Methyl malonic acid				√	
4	3,31	2-Propenoic acid				√	
5	4,23	Acrylic Acid					√
6	4,78	Lactic acid				√	√
7	4,88	2,4,5-trimethyl-1,3-doixolane				√	
8	6,18	2,5-Furandione, 3-methyl				√	
9	6,54	Benzene derivative					√
10	7,12	2,5-Furandione, 3,4-dimethyl				√	√
11	7,39	Hexanal				√	√
12	8,04	l/d-Lactide	√	√	√	√	√
13	8,41	l/d-Lactide	√	√	√	√	√
14	8,48	Decanol			√	√	√
15	8,53	2H-Pyran-2-one, tetahydro-5,6-dimethyl-trans					√
16	9,05	m-Toluic acid					√
17	9,44	Anhydride Ftalic	√	√	√	√	√
18	9,97	Biphenyl	√	√	√	√	√
19	10,34	Diethyl maleate/1H-isoindole-1,3(2H)dione-2metil	√	√	√	√	√
20	10,65	1H-Isoindole-1,3(2H)dione	√	√	√	√	√
21	12,12	Aromatic derivative				√	√
22	13,36	9H-Fluoren-one	√	√	√	√	√
23	13,72	Antracene	√	√	√	√	√
24	13,84	9H-Fluorene, 9 methylene					
25	14,39	1-Methyl triciclo (2.2.1.1(2,6)heptane)					√
26	14,49	Pyrene, 4,5-dihydro	√	√	√	√	√
27	14,73	Pyrene derivative	√	√	√	√	√
28	14,85	Anthracene, 1-methyl	√	√	√	√	√
29	14,91	Anthracene, 2-methyl	√	√	√	√	√
30	15,35	2-Phenyl naphthalene	√	√	√	√	√
31	15,41	Pyrene derivative	√	√	√	√	√
32	16,42	Pyrene derivative	√	√	√	√	√
33	17,14	p-terphenyl	√	√	√	√	√
34	17,50	Aromatic derivative	√	√	√	√	√

PLA-W							
Peak	T_R	Compound	175ºC	230ºC	300ºC	450ºC	600ºC
1	2,44	Acetic Acid				√	√
2	2,85	2,3-Pentanedione				√	√
3	4,23	Acrylic Acid				√	√
4	4,78	Lactic acid				√	√
5	4,88	Isómero del anterior				√	√
6	6,54	Benzene derivative				√	√
7	7,12	2,5-Furandione, 3,4-dimethyl				√	√
8	7,39	Hexanal				√	√
9	8,04	l/d-Lactide	√	√	√	√	√
10	8,41	l/d-Lactide	√	√	√	√	√
11	8,48	Decanol			√		
12	8,59	3-Methyl butyrolactone				√	√
13	9,05	m-Toluic acid					√
14	9,44	Anhydride Ftalic	√	√	√	√	√
15	9,97	Biphenyl	√	√	√	√	√
16	10,34	Diethyl maleate/1H-isoindole-1,3(2H)dione-2metil	√	√	√	√	√
17	10,65	1H-Isoindole-1,3(2H)dione	√	√	√	√	√
18	11,88	Benzoic acid derivative					√
19	12,12	Aromatic derivative				√	√
20	13,36	9H-Fluoren-one	√	√	√	√	√
21	13,72	Antracene	√	√	√	√	√
22	13,84	9H-Fluorene, 9-methylene	√	√	√	√	√
23	14,49	Pyrene, 4,5-dihydro	√	√	√	√	√
24	14,73	Pyrene derivative	√	√	√	√	√
25	14,85	Anthracene, 1-methyl	√	√	√	√	√
26	14,91	Anthracene, 2-methyl	√	√	√	√	√
27	15,41	Pyrene derivative	√	√	√	√	√
28	16,42	Pyrene derivative	√	√	√	√	√
29	16,64	Naphthalene, 2-(phenylmethyl)	√	√	√	√	√
30	17,14	p-terphenyl	√	√	√	√	√
31	17,50	Aromatic derivative	√	√	√	√	√

E.P.							
Peak	T_R	Compound	175ºC	230ºC	300ºC	450ºC	600ºC
1	2,13	Butanone				√	√
2	2,44	Acetic Acid				√	√
3	2,85	2,3-Pentanedione				√	√
4	4,23	Acrylic Acid				√	√
5	4,78	Lactic acid				√	√
6	5,29	2-Propenone,1-(acetyloxy)				√	√
7	6,09	2-Cyclopenten-1-one, 3,4-dimethyl				√	√
8	6,37	2-butanone,1-(acetyloxy)				√	√
9	7,30	Etoxyethene				√	√
10	7,39	Hexanal				√	√
11	8,04	l/d-Lactide	√	√	√	√	√
12	8,41	l/d-Lactide	√	√	√	√	√
13	9,44	Anhydride Phtalic	√	√	√	√	√
14	9,97	Biphenyl	√	√	√	√	√
15	10,34	Diethyl maleate/1H-isoindole-1,3(2H)dione-2metil	√	√	√	√	√
16	10,65	1H-Isoindole-1,3(2H)dione	√	√	√	√	√
17	11,88	Benzoic acid derivative					√
18	12,12	Aromatic derivative				√	√
19	13,36	9H-Fluoren-one	√	√	√	√	√
20	13,72	Antracene	√	√	√	√	√
21	13,84	9H-Fluorene, 9-methylene	√	√	√	√	√
22	14,13	Tricyclo (2.2.2.0.1.4) octane					√
23	14,41	1-Methyltricyclo (2,1,1,0 (2,6))heptane					√
24	14,49	Pyrene, 4,5-dihydro	√	√	√	√	
25	14,73	Pyrene derivative					√
26	14,85	Anthracene, 1-methyl	√	√	√	√	√
27	14,91	Anthracene, 2-methyl	√	√	√	√	
28	15,54	2-Phenyl naphthalene	√	√	√	√	√
29	16,42	Pyrene derivative	√	√	√	√	√
30	16,64	Naphthalene, 2-(phenylmethyl)	√	√	√	√	√
31	17,14	p-terphenyl	√	√	√	√	√
32	17,50	Aromatic derivative	√	√	√	√	√

PETG							
Peak	T_R	Compound	175ºC 30 s	230ºC 30 s	300ºC 30 s	450ºC 30 s	600ºC 30s
1	2,56	Benzene					√
2	3,91	Toluene					√
3	4,54	Cyclohexane,1,4-bis-(methylene)					√
4	5,05	Octa-2,4,6-triene					√
5	5,17	1,5-Dimethyl-1,4-cyclohexadiene					√
6	5,29	m-Xylene					√
7	5,56	1,4-Cyclohexadiene 1,2-dimethyl					√
8	6,35	Benzene (1-methylethyl)					√
9	6,67	1,2,3-trimethylbenzene					√
10	6,71	Benzene derivative					√
11	7,08	3-Cyclohexene-1-carboxaldehyde, 4-methyl					√
12	7,51	p-Tolualdehyde					√
13	7,95	Ethylphenylglyoxylate					√
14	8,60	Benzoic acid					√
15	8,91	1-Propanone, 2-methyl-1-(2-methylphenyl)					√
16	9,15	p-Toluic acid					√
17	9,85	Vinyl trans-cinnamate					√
18	11,08	p-Diacetyl benzene					√
19	11,28	Terephtalic acid, methyl vinyl ester					√
20	11,59	2,4-Imidazolidinedione					√
21	11,98	Phtalic acid, cyclobutylethylester					√
22	14,13	Cyclohexane 1,4-bis (methylene)					√
23	14,39	Octa-2,4,6-triene					√